

## Scalable Routes to Janus Au–SiO<sub>2</sub> and Ternary Ag–Au–SiO<sub>2</sub> Nanoparticles

Tao Chen,<sup>†</sup> Gang Chen,<sup>†</sup> Shuangxi Xing,<sup>†</sup> Tom Wu,<sup>‡</sup> and Hongyu Chen<sup>\*†</sup>

<sup>†</sup>Division of Chemistry and Biological Chemistry and  
<sup>‡</sup>Division of Physics and Applied Physics, Nanyang  
Technological University, 21 Nanyang Link, 637371,  
Singapore

Received April 25, 2010

Revised Manuscript Received May 30, 2010

Janus particle has become a focus of attention in materials science since the first emphasis by Gennes in his Nobel Prize address.<sup>1</sup> Generally, Janus particles possess dual surface functionalities or consist of two jointed components with distinct properties.<sup>2</sup> The integration of different nanomaterials with semiconducting, magnetic or plasmonic properties permits versatile applications ranging from biosensing, drug delivery to catalysis.<sup>3</sup> On the other hand, the noncentrosymmetric arrangement of components allows specific organizations of Janus particles into well-defined architectures such as dimers, trimers, or helices.<sup>4</sup>

During the past decades, considerable efforts have been devoted to the fabrication of Janus particles.<sup>2</sup> For instance, toposelective functionalization has been demonstrated to be an effective approach toward Janus particles.<sup>2b</sup> Initially, bulk solid substrates were used to support a monolayer of spherical particles such as those of polystyrene or silica.<sup>5</sup> Thus, the functionalization could take place only on the top surfaces of the anchored particles. Because the limited surface area of a bulk substrate often led to low yield of Janus particles, a modified method was later adapted by using

colloidal particles<sup>6</sup> as the supporting substrates. Another method for synthesizing Janus particles was carried out at interfaces. As such, a particle in partial contact with a reactive medium generated different surface functionalities on the opposite surfaces.<sup>6c</sup> Taking advantage of microfluidic technique, Janus particles could be consecutively fabricated by solidifying droplets composed of immiscible components.<sup>7</sup> Other methods such as controllable polymer attachment,<sup>8</sup> phase separation,<sup>9</sup> and controlled surface nucleation<sup>10</sup> were also adapted to produce Janus particles.

Although the previously reported cases of Janus particles were often close to micrometer in size and typically involved various types of polymers, the fabrication of small Janus nanoparticles (< 100 nm) with inorganic materials presents a greater challenge.<sup>10</sup> On the other hand, silica is a widely used material for building concentric core–shell structures with cores such as metallic or magnetic nanoparticles or quantum dots,<sup>11</sup> but so far there has been no report of Janus nanoparticles with partial silica shells. Because of the amorphous nature of silica, it is often difficult to fine-tune the surface tension or lattice mismatch between silica and these core materials. Herein, we developed a new approach to control silica deposition on partial surface of Au nanospheres (NSs). The selective deposition was driven by the partitioned surface functionalities on AuNSs through competitive ligand coordination (Figure 1). The partial silica shells reduced the symmetry of the AuNSs while keeping the cores available for further modification. Thus, AgNSs or Ag nanorods (NRs) were grown on the exposed Au surface, generating ternary Ag–Au–SiO<sub>2</sub> structures and further reducing the symmetry.

In a typical synthesis of the Janus Au–SiO<sub>2</sub> nanostructures, 4-mercaptophenylacetic acid (4-MPAA) and poly(acrylic acid) (PAA<sub>86</sub>,  $M_w = 6200$ ; [4-MPAA]/[PAA<sub>86</sub>] = 1:0.129) were employed as the competing ligands to

\*Corresponding author. E-mail: hongyuchen@ntu.edu.sg. Fax: (+65) 67911961. Tel: (+65) 65138795.

- (1) de Gennes, P. G. *Rev. Mod. Phys.* **1992**, *64*, 645.
- (2) (a) Walther, A.; Müller, A. H. E. *Soft Matter* **2008**, *4*, 663. (b) Perro, A.; Reculusa, S.; Ravaine, S.; Bourgeat-Lami, E. B.; Duguet, E. *J. Mater. Chem.* **2005**, *15*, 3745. (c) Casagrande, C.; Fabre, P.; Raphaël, E.; Veysie, M. *Europhys. Lett.* **1989**, *9*, 251. (d) Xu, C. J.; Wang, B. D.; Sun, S. H. *J. Am. Chem. Soc.* **2009**, *131*, 4216. (e) Binks, B. P. *Curr. Opin. Colloid Interface Sci.* **2002**, *7*, 21. (f) Chen, T.; Wang, H.; Chen, G.; Wang, Y.; Feng, Y. H.; Teo, W. S.; Wu, T.; Chen, H. Y. *ACS Nano* **2010**. DOI:10.1021/nn100269v.
- (3) (a) Wang, C.; Daimon, H.; Sun, S. H. *Nano Lett.* **2009**, *9*, 1493. (b) Roh, K. H.; Martin, D. C.; Lahann, J. *Nat. Mater.* **2005**, *4*, 759. (c) Xu, C. J.; Xie, J.; Ho, D.; Wang, C.; Kohler, N.; Walsh, E. G.; Morgan, J. R.; Chin, Y. E.; Sun, S. H. *Angew. Chem., Int. Ed.* **2008**, *47*, 173.
- (4) (a) Zerrouki, D.; Baudry, J.; Pine, D.; Chaikin, P.; Bibette, J. *Nature* **2008**, *455*, 380. (b) Hong, L.; Cacciuto, A.; Luijten, E.; Granick, S. *Nano Lett.* **2006**, *6*, 2510.
- (5) (a) Cayre, O.; Paunov, V. N.; Velev, O. D. *J. Mater. Chem.* **2003**, *13*, 2445. (b) Pawar, A. B.; Kretschmar, I. *Langmuir* **2008**, *24*, 355. (c) Lu, Y.; Xiong, H.; Jiang, X. C.; Xia, Y. N.; Prentiss, M.; Whitesides, G. M. *J. Am. Chem. Soc.* **2003**, *125*, 12724.
- (6) (a) Hong, L.; Jiang, S.; Granick, S. *Langmuir* **2006**, *22*, 9495. (b) Huo, F. W.; Lytton-Jean, A. K. R.; Mirkin, C. A. *Adv. Mater.* **2006**, *18*, 2304. (c) Pradhan, S.; Xu, L. P.; Chen, S. W. *Adv. Func. Mater.* **2007**, *17*, 2385. (d) Jiang, S.; Granick, S. *Langmuir* **2008**, *24*, 2438. (e) Perro, A.; Meunier, F.; Schmitt, V.; Ravaine, S. *Colloid Surf., A* **2009**, *332*, 57.
- (7) (a) Nisisako, T.; Torii, T.; Takahashi, T.; Takizawa, Y. *Adv. Mater.* **2006**, *18*, 1152. (b) Nie, Z. H.; Li, W.; Seo, M.; Xu, S. Q.; Kumacheva, E. *J. Am. Chem. Soc.* **2006**, *128*, 9408.
- (8) (a) Ohnuma, A.; Cho, E. C.; Camargo, P. H. C.; Au, L.; Ohtani, B.; Xia, Y. *J. Am. Chem. Soc.* **2009**, *131*, 1352. (b) Chen, T.; Yang, M. X.; Wang, X. J.; Tan, L. H.; Chen, H. Y. *J. Am. Chem. Soc.* **2008**, *130*, 11858. (c) Qiang, W.; Wang, Y.; He, P.; Xu, H.; Gu, H.; Shi, D. *Langmuir* **2008**, *24*, 606. (d) Tan, L. H.; Xing, S. X.; Chen, T.; Chen, G.; Huang, X.; Zhang, H.; Chen, H. Y. *ACS Nano* **2009**, *3*, 3469.
- (9) (a) Shah, R. K.; Kim, J. W.; Weitz, D. A. *Adv. Mater.* **2009**, *21*, 1949. (b) Liu, Y. F.; Abetz, V.; Müller, A. H. E. *Macromolecules* **2003**, *36*, 7894. (c) Gu, H. W.; Zheng, R. K.; Zhang, X. X.; Xu, B. *J. Am. Chem. Soc.* **2004**, *126*, 5664.
- (10) (a) Shi, W. L.; Zeng, H.; Sahoo, Y.; Ohulchanskyy, T. Y.; Ding, Y.; Wang, Z. L.; Swihart, M.; Prasad, P. N. *Nano Lett.* **2006**, *6*, 875. (b) Wei, Y. H.; Klajn, R.; Pinchuk, A. O.; Grzybowski, B. A. *Small* **2008**, *4*, 1635. (c) Yang, J.; Elim, H. I.; Zhang, Q.; Lee, J. Y.; Ji, W. *J. Am. Chem. Soc.* **2006**, *128*, 11921. (d) Gu, H. W.; Yang, Z. M.; Gao, J. H.; Chang, C. K.; Xu, B. *J. Am. Chem. Soc.* **2005**, *127*, 34. (e) Wang, C.; Wei, Y. J.; Jiang, H. Y.; Sun, S. H. *Nano Lett.* **2009**, *9*, 4544. (f) Yang, J.; Peng, J. J.; Zhang, Q. B.; Peng, F.; Wang, H. J.; Yu, H. *Angew. Chem., Int. Ed.* **2009**, *48*, 3991. (g) Glaser, N.; Adams, D. J.; Boker, A.; Krausch, G. *Langmuir* **2006**, *22*, 5227.
- (11) (a) Liz-Marzán, L. M.; Giersig, M.; Mulvaney, P. *Langmuir* **1996**, *12*, 4329. (b) Stöber, W.; Fink, A.; Bohn, E. *J. Colloid Interface Sci.* **1968**, *26*, 62. (c) Selvan, S. T.; Patra, P. K.; Ang, C. Y.; Ying, J. Y. *Angew. Chem., Int. Ed.* **2007**, *46*, 2448.

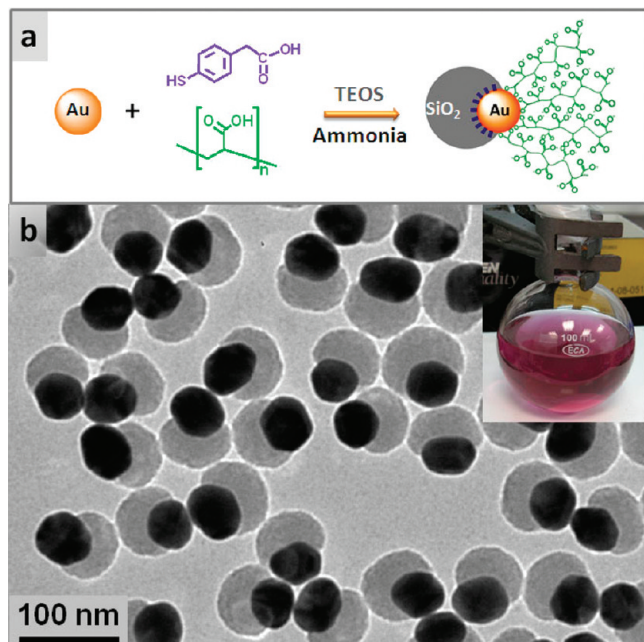


**Figure 1.** (a) Schematic illustration of the ligand competition that led to the formation of Janus Au-SiO<sub>2</sub>; (b) TEM image of Janus Au-SiO<sub>2</sub>, with [4-MPAA]:[PAA<sub>86</sub>] = 1:0.129 and [TEOS] = 1.445 mM; inset, a digital photo showing the product of a scaled-up synthesis (72 mL).

functionalize citrate-stabilized AuNSs ( $d_{\text{avg}} = 44$  nm) in 2-propanol/water (5:1, v/v) mixture. Tetraethyl ortho-silicate (TEOS) was used as silica precursor. After its hydrolysis and subsequent condensation catalyzed by ammonia, the surface of the AuNSs was partially encapsulated with SiO<sub>2</sub> (Figure 1b). Nearly all AuNSs (> 99%) had partial shells and the Janus structure was highly uniform. After etching the Au cores, the resulting product showed silica nanobowls with openings (Figure 2a, in cases with right perspective), indicating that the “exposed” Au surface was indeed not covered with silica.

This method can be adapted for synthesizing other types of Janus nanoparticles with either a different ligand combination (16-mercaptohexadecanoic acid and PAA<sub>86</sub>) or a different metal core (AuNR).<sup>12</sup> The utilization of ligand competition to regulate anisotropic silica deposition was inspired by our previous success in the synthesis of Janus Au-PSPAA nanoparticles (PSPAA: polystyrene-*block*-poly(acrylic acid)), where two types of ligands were found to segregate on the surface of Au nanoparticles and thus directed the polymer self-assembly.<sup>8b,d</sup> In comparison, the regioselective deposition of silica presents a different challenge that involves the manipulation of metal–ligand–silica interfaces.

To investigate the roles of the two ligands, we carried out the silica deposition by using either 4-MPAA or PAA<sub>86</sub> separately. When 4-MPAA was utilized as the sole ligand, similar synthesis gave rise to concentric Au-SiO<sub>2</sub> core–shell structure in nearly all AuNSs (> 99%, Figure 2b). The full encapsulation was likely a result of the surface carboxylic groups after 4-MPAA adsorption which rendered the AuNS surface

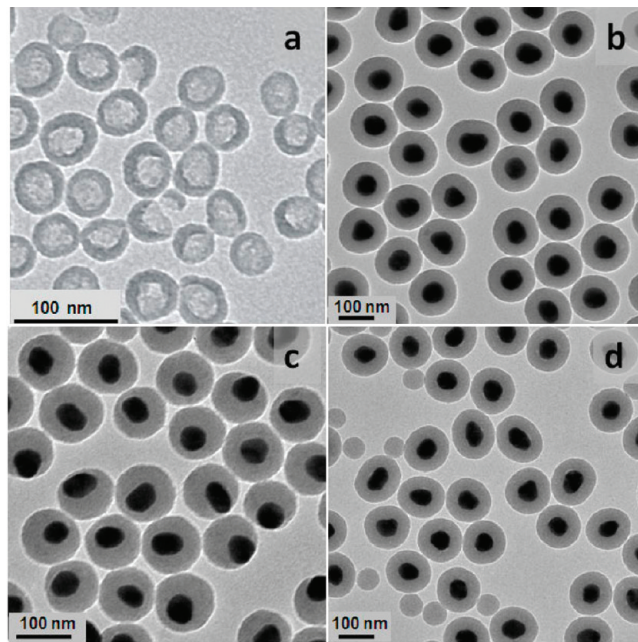


**Figure 2.** TEM images of (a) open silica bowls produced by removing Au cores from the Janus Au-SiO<sub>2</sub> nanoparticles in Figure 1b; (b) concentric Au-SiO<sub>2</sub> prepared with [4-MPAA]:[PAA<sub>86</sub>] = 1:0; (c) eccentric Au-SiO<sub>2</sub> prepared with [4-MPAA]:[PAA<sub>86</sub>] = 1:0.065; and (d) concentric Au-SiO<sub>2</sub> prepared using only acrylic acid as ligand.

vitrophilic.<sup>13</sup> On the other hand, when PAA was used as the sole ligand, AuNSs were not encapsulated. Therefore, the formation of Janus Au-SiO<sub>2</sub> possibly resulted from segregated coordination<sup>14</sup> of 4-MPAA and PAA on the AuNS surface, which then directed silica deposition (Figure 1a). Surface-enhanced Raman scattering (SERS) signal of 4-MPAA from the Janus Au-SiO<sub>2</sub> is weaker than that of the concentric Au-SiO<sub>2</sub> based on the same AuNSs concentrations (Figure 3a, b). Because neither of these two samples was aggregated on the basis of UV–vis spectra,<sup>12</sup> the SERS results confirmed that 4-MPAA probably did not fully cover the Au surface in the Janus Au-SiO<sub>2</sub> as a result of the PAA competition. Furthermore, at lower PAA concentration ([4-MPAA]:[PAA<sub>86</sub>] = 1:0.065), the resulting nanoparticles showed eccentric Au-SiO<sub>2</sub> structures (Figure 2c). Though not all of these particles were oriented at a right direction to reveal the exposed Au surface, it is obvious that the exposed surface was smaller than that of the Janus Au-SiO<sub>2</sub> in Figure 1b. The fact that the [4-MPAA]:[PAA<sub>86</sub>] ratio affected the silica deposition strongly supports the ligand competition theory.

Further control experiments demonstrated that when the monomer of PAA, i.e., acrylic acid, was used as the ligand, concentric Au-SiO<sub>2</sub> nanoparticles (Figure 2d) were obtained under otherwise the same conditions. Thus, the fact that the PAA-stabilized AuNSs were not able to support silica is probably owing to the polymeric nature of PAA. Though carboxylate-functionalized metal surfaces were known to be amenable to silica deposition,<sup>13</sup> 4-MPAA, PAA and acrylic acid all contain carboxylate groups. The polymer layer could

(12) See the Supporting Information for details.

(13) (a) Wallace, A. F.; DeYoreo, J. J.; Dove, P. M. *J. Am. Chem. Soc.* **2009**, *131*, 5244. (b) Xue, C.; Chen, X.; Hurst, S. J.; Mirkin, C. A. *Adv. Mater.* **2007**, *19*, 4071.

(14) Love, J. C.; Estroff, L. A.; Kriebel, J. K.; Nuzzo, R. G.; Whitesides, G. M. *Chem. Rev.* **2005**, *105*, 1103.

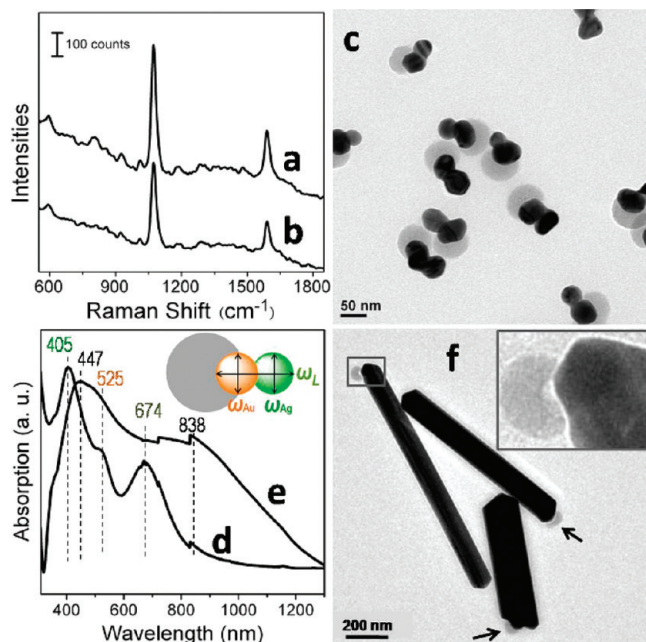


**Figure 3.** (a, b) SERS spectra of the concentric Au-SiO<sub>2</sub> in Figure 2b and the Janus Au-SiO<sub>2</sub> in Figure 1b, respectively; (c, d) TEM image and UV-vis-NIR absorption spectrum of the ternary structures AgNS-Au-SiO<sub>2</sub>; inset, possible plasmon resonance modes of the Au-Ag heterodimers; (e, f) UV-vis-NIR spectrum and TEM image of AgNR-Au-SiO<sub>2</sub>; inset in f, high-magnification image of an end of AgNR-Au-SiO<sub>2</sub>.

block the diffusion of TEOS to the Au surface<sup>15</sup> and, more importantly, the high solubility of PAA in the solution led to small PAA-solution interfacial energy, which is unfavorable for heterogeneous silica nucleation (for the same reason homogeneous nucleation of silica in the solution is unfavorable). In contrast, with small molecules as ligands, the Au-ligand-solution interface has high energy,<sup>15</sup> making such a surface prone to silica deposition.

To exploit the Janus conformation, we fabricated ternary Ag-Au-SiO<sub>2</sub> nanostructures using the purified Janus Au-SiO<sub>2</sub> nanoparticles as seeds (Figure 3c, f). AgNO<sub>3</sub> was added dropwise to an aqueous mixture of hydroquinone (HQ) and polyvinylpyrrolidone (PVP), which were used as reductant and stabilizing agent, respectively. Upon AgNO<sub>3</sub> addition, the color of the solution changed from red to yellow and finally to brown, indicating that the formation of Au-Ag hybrid structures has altered the plasmon resonance of the original AuNSs (Figure 3d). The fast reduction of AgNO<sub>3</sub> by HQ<sup>16</sup> minimized the infiltration of AgNO<sub>3</sub> through the silica shell, favoring Ag growth on the exposed Au surface. This heterogeneous nucleation of Ag also prevented the formation of freestanding AgNSs from homogeneous nucleation.<sup>16</sup>

The facile preparation of the jointed Au-Ag heterodimer is of significance.<sup>10d</sup> Since Ag and Au have close lattice constants, Ag readily coats Au seeds during its nucleation. Most of the previously reported Au-Ag

hybrids were core-shell structures where one metal completely coated the other.<sup>17</sup> In our colloidal ternary Ag-Au-SiO<sub>2</sub> nanoparticles, the juxtaposition of AuNSs and AgNSs led to interesting optical properties.<sup>18</sup> Their transverse plasmon resonance absorption peaks occurred at 525 and 405 nm, respectively, consistent with those of freestanding NSs. In addition, an absorption peak at 674 nm could be assigned to the longitudinal plasmon coupling between the AuNS and AgNS (Figure 3d).<sup>18</sup> This wavelength was larger than that of AgNS dimers (~560 nm) but close to that of AuNS dimers of smaller sizes.<sup>19</sup>

The affinity of PVP to Ag {100} and {111} facets is well-known for guiding the growth of nanocubes and NRs.<sup>20</sup> In contrast to the incompatibility of PVP with PSPAA,<sup>8b,d</sup> silica shells were perfectly stable in the presence of PVP. This gave rise to an interesting opportunity to control the facets of Ag blocks in hybrid nanostructures (Figure 3f). Upon extensive Ag growth on Janus Au-SiO<sub>2</sub> seeds, the Ag blocks developed into rod shapes with regular and parallel facets indicating internal lattice order. The Au absorption peak was masked, leaving transverse and longitudinal absorption peaks of Ag at 447 and 838 nm, respectively (Figure 3e). The silica shell always occurred at the ends of the AgNRs, suggesting the significant role played by the partially exposed Au seeds. Interestingly, the extensive growth of Ag seemed to have dragged the AuNSs out from the silica shells in some cases (about 20%, Figure 3f). Because the nanoparticles may not have oriented at a right perspective to reveal the resulting cavity in all cases, the actual occurrence could be somewhat higher. Similar phenomenon was observed previously in the overgrowth of Au on Janus Au-Fe<sub>3</sub>O<sub>4</sub> nanoparticles.<sup>10e</sup>

In summary, we demonstrated new routes to hybrid nanostructures with reduced symmetry. The capability to direct silica deposition by controlling ligand distribution on metallic nanoparticles may be extended to other core-shell systems. With the previous success in those systems, it could be expected that a broad range of complex hybrid nanoparticles could be fabricated by similar colloidal approaches. Their scalable fabrication will aid future efforts in assembling nanodevices and exploring novel properties.

**Acknowledgment.** The authors thank Ministry of Education, Singapore (ARC 27/07 and 13/09), for financial support.

**Supporting Information Available:** Experimental details, UV-vis absorption spectra, and large view of TEM images (PDF). This material is available free of charge via the Internet at <http://pubs.acs.org>.

(15) Mann, S., *Biomineralization—Principles and Concepts in Bioinorganic Materials Chemistry*; Oxford University Press: New York, 2001; Vol. 1.

(16) Gentry, S. T.; Fredericks, S. J.; Krchnavek, R. *Langmuir* **2009**, *25*, 2613.

(17) (a) Hu, K. W.; Liu, T. M.; Chung, K. Y.; Huang, K. S.; Hsieh, C. T.; Sun, C. K.; Yeh, C. S. *J. Am. Chem. Soc.* **2009**, *131*, 14186. (b) Xie, W.; Su, L.; Donfack, P.; Shen, A.; Zhou, X.; Sackmann, M.; Materny, A.; Hu, J. *Chem. Commun.* **2009**, 5263.

(18) Ghosh, S. K.; Pal, T. *Chem. Rev.* **2007**, *107*, 4797.

(19) (a) Chen, G.; Wang, Y.; Yang, M.; Xu, J.; Goh, S. J.; Pan, M.; Chen, H. *J. Am. Chem. Soc.* **2010**, *132*, 3644. (b) Chen, G.; Wang, Y.; Tan, L. H.; Yang, M.; Tan, L. S.; Chen, Y.; Chen, H. *J. Am. Chem. Soc.* **2009**, *131*, 4218.

(20) Wiley, B.; Sun, Y. G.; Mayers, B.; Xia, Y. N. *Chem. Eur. J.* **2005**, *11*, 454.